Original Research Article

Electrochemical Studies on the Corrosion Behavior of Mild Steel in NaCl Aqueous Solutions with Zinc Ions.

ABSTRACT

The corrosion behaviors of mild steel in NaCl aqueous solution with different Zn^{2+} concentrations have been investigated electrochemically. The immersion potentials were influenced by the presence of Zn^{2+} and were shifted to the positive direction with increasing the Zn^{2+} concentration in the solutions. Zn^{2+} suppressed the current density in both cathodic and anodic polarization and the inhibition effects were increased with increasing the Zn^{2+} concentrations. The electrochemical impedance spectroscopy (EIS) results showed the highest charge transfer resistance in the Zn-rich solution due to the formation of Zn-layer with the steel surface. The Zn-layer thickness was increased and the area of defects in the oxide film on the steel surface was decreased with increasing the Zn^{2+} concentration. Therefore, it was suggested that the corrosion inhibition ability of mild steel in NaCl aqueous solution was significantly improved with increasing the concentration of Zn^{2+} in the solution.

Keywords: mild steel; corrosion; electrochemical test; polarization; EIS.

1. INTRODUCTION

Modern civilization is growing up with advanced constructions. Many engineers and architects prefer steel over wood, glass and other materials for construction purposes due to its durability, unerring strength, pliability and sustainability. Mild steels are one of the good choices for the consumers that abundantly used in many areas. However, mild steels are not corrosion resistant and corrosion of these steels is a global problem that randomly occurring in a wide range of areas such as seawater environment [1-3], acid environment [4, 5] and in concentrated NaCl environment [6]. There are numbers of studies have been carried out regarding mild steel corrosion [7, 8] in natural extract [9], in acid solution [10-13] and in chloride aqueous solutions [14]. Composition of the oxide film that is formed on the steel surface is very much important and plays a significant role in the corrosion inhibition in aqueous solutions. It is recognized that chloride ions are very much aggressive and have a tendency to destroy the oxide film by film thinning, penetration and film rupture mechanisms [14-19]. Usually, metal dissolution is initiated after the destruction of oxide film by the chloride ions [20-23]. Oxide film destruction rate is increased with increasing the chloride ion concentration. Consequently, the metal dissolution rate is also increased [24, 25].

It is quite difficult to prevent the corrosion of steel hundred per cent. However, consumers are always trying to control the corrosion as much as conceivable. Coatings and organic-inorganic inhibitors are often used to diminish the corrosion percentage. There are so many environmental laws have been forced on the use of non-toxic and low-cost materials as corrosion inhibitors. This assortment has encouraged many researchers to discover some inhibitors that will have extensive consideration due to their properties like as environment-friendly, low influence on the human body, low cost, easy to handle and renewability. There are several studies have been carried out that metal cations have a tendency to inhibit the corrosion of steel in aqueous solutions as metal cations are available, low cost and easy to handle. There are some researchers [20-23, 26, 27] reported that Zn^{2+} inhibited the corrosion of steel in aqueous solutions by forming a layer with the steel surface. Drazic *et al*. [28] explained that the hydrogen evaluation reaction rate was suppressed by Zn^{2+}, Cd^{2+}, and Mn^{2+} in H_2SO_4 solution and thus corrosion of iron was inhibited. Some nuclear power plant uses Zn^{2+} to control the corrosion of reactor component materials [29]. Several researchers [30-35] also reported that Zn^{2+} significantly enhanced the inhibition performance of some traditional corrosion inhibitors. Thebault *et al*. [36] stated that Zn^{2+} is more effective than Mg^{2+} to inhibit the cathodic reactions on the

steel surface in 0.03 M NaCl solution. Tada *et al*. [37] showed that Zn^{2+} inhibited the cathodic reaction on Zn/Steel couple in 0.01 M NaCl solution. Sakairi *et al*. [38] elucidated that after laser irradiation, the rest potential changes negative to positive direction while the zinc-coated layer is exposed in the 0.01 kmol m^{-3} NaCl solution. Hirasaki *et al*. [39] stated that the anodic current was decreased with increasing the Zn^{2+} concentration in the acid solution.

It has been recognized that Zn^{2+} appreciably inhibit the corrosion of steels in aqueous chloride solutions. However, the situation of stepwise increasing the zinc ion on the corrosion behavior of mild steel in chloride solution was not focused in the view of electrochemical measures. It is still not fully elucidated the electrochemical behavior and corrosion mechanism of mild steel in NaCl aqueous solution in the presence of Zn^{2+} with different concentrations. The present research purpose is to clarify the corrosion behavior of mild steel in NaCl aqueous solution with different concentrations of Zn^{2+} by electrochemical techniques.

2. MATERIAL AND METHODS

2.1 Testing Samples

Mild steel sheet with 0.7 mm thickness (composition by mass%: C = 0.02; Mn = 0.18; P = 0.015; S < 0.01; and Fe = balance) was used as the sample for this experiment. The mild steel sheet was cut into 7 × 7 mm in size and it was connected to a Cu wire. Each sample was embedded in epoxy resin leaving one side exposed surface.

SiC abrasive paper was used to abrade the exposed surface of the sample from 400 to 4000 grit size. The samples were cleaned in an ultrasonic bath with ethanol and highly purified water before the tests.

2.2 Experimental solutions

The solutions of Zn^{2+} were prepared from $ZnCl_2$. Three different concentration of Zn^{2+} solutions as 0.1 mol m^{-3} $ZnCl_2$ (Zn_{Sol-L}), 0.5 mol m^{-3} $ZnCl_2$ (Zn_{Sol-M}) and 1.0 mol m^{-3} $ZnCl_2$ (Zn_{Sol-H}) were prepared together with 10 mol m^{-3} NaCl (Na_{sol}). The Cl^- concentration of all solutions was adjusted to 10 mol m^{-3} by NaCl. The 10 mol m^{-3} NaCl was used as the reference solution. The experimental solutions were prepared by highly purified water (MILLIPORE, Simplicity UV). All the solutions were colorless and transparent before the tests. The pH of the solutions was around neutral. All of the chemicals used in this experiment were special grade from Kanto Chemical Co. Ltd.

2.3 Electrochemical measurements

Electrochemical measurements were carried out at 25°C in a conventional three-electrode cell system using a computer-controlled potentiostat (IVIUM TECHNOLOGIES, Pocketstat). The exposed surface area of specimens in the solution was 0.49 cm^2. Specimens were immersed in the solutions for 1 h at 25°C before the tests. A Ag/AgCl electrode (SSE) immersed in a saturated KCl solution was used as the reference electrode and a Pt plate was used as the counter electrode. The potentiodynamic polarization measurements were carried out from immersion potential to the cathodic and anodic direction with a scan rate of 60 mV/minute. The cathodic and anodic scans were recorded individually to obtain the specific electrochemical properties of mild steel immersed in the solutions with different concentrations of Zn^{2+}. The electrochemical impedance spectroscopy (EIS) measurements were carried out at open circuit potential in the frequency range from 10 kHz to 1 mHz and modulation amplitude of 10 mV. Each measurement was performed with three replicates and reproducible data were obtained. The EIS data were analyzed by a software called IVIUM.

3. RESULTS AND DISCUSSION

3.1 Immersion Potential

The changes in immersion potentials of the specimens with the Zn^{2+} concentration in the solutions for 1 h at room temperature are shown in Fig. 1. In all the cases, the potentials are decreased with time. All the measured values of potentials are confined in a range between -0.2 V and -0.41 V, and only slight differences can be noticed. After 3000 s of immersion, all the potentials reach a stable value, and the Na_{sol} shows the lowest potential as compared to the other solutions. The immersion potentials are shifted to a positive direction with increasing the Zn^{2+} concentration in the solutions. These results suggest that Zn^{2+} has a significant influence on the immersion potential of the specimen in the solutions.

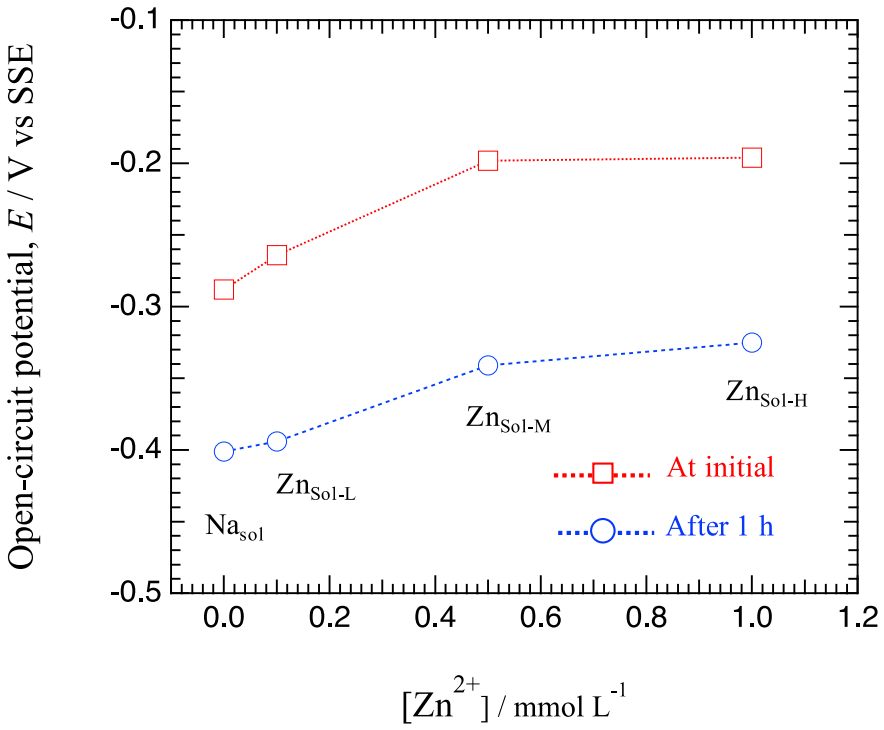

Fig. 1 Changes in open-circuit potential with Zn^{2+} concentration in the solutions for 1 h at room temperature.

3.2 Polarizations measurement

The cathodic and anodic polarization behaviors were observed in different solutions and are shown in Fig. 2. In the cathodic polarization curves, at around -0.8 V, the lowest current density is observed in the Zn rich solution (Zn_{Sol-H}). The highest current density is observed in the Na_{Sol} as compared to the other solutions. In the anodic polarization curves, at around -0.15 V, the lowest current density is observed in the Zn rich solution (Zn_{Sol-H}) as compared to the other solutions. The highest current density is also observed in the Na_{Sol} as compared to the other solutions. The polarization behavior demonstrates that the presence of Zn^{2+} suppresses the current density in both cathodic and anodic polarization, and the inhibition effect is increased with increasing the Zn^{2+} concentration in the solutions.

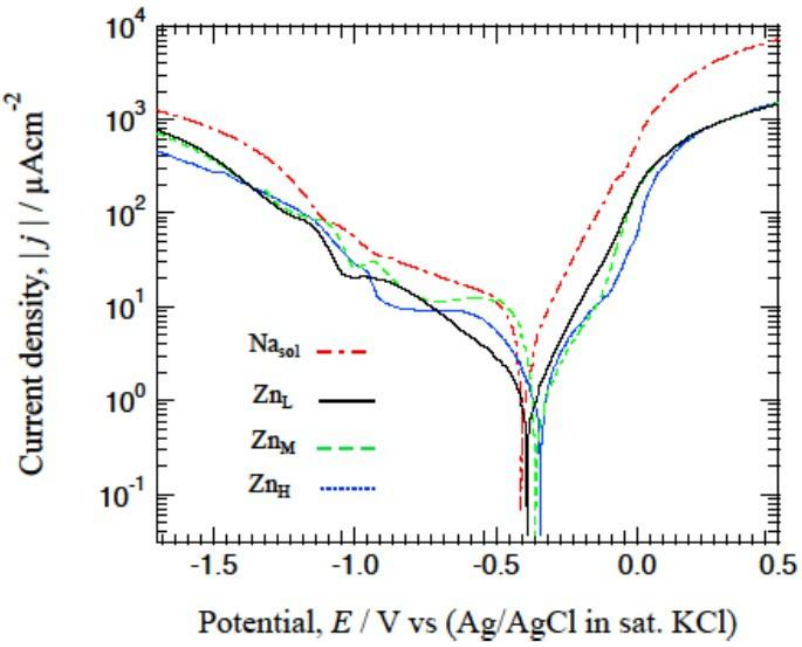

Fig. 2 Potentiodynamic cathodic and anodic polarization curves after immersion in the solutions for 1 h at room temperature.

3.3 EIS measurements

EIS measurements were carried out at room temperature. Before the measurement, samples were immersed in the solution for 1 h. Figs. 3 a), b) and c) show the Bode diagram of impedance, phase shift plot, and Nyquist plot respectively. The fitted lines are also shown in Figs. 3 a), b) and c) which were calculated by an equivalent circuit shown in Fig. 4. The equivalent circuit pretends an electrode with a protective film having a defect [35, 40]. The equivalent circuit consists (Fig. 4) of bulk solution resistance (R_{sol}), solution resistance of the defects in the protective film (R_d), charge transfer resistance of metal dissolution at the metal/solution interface inside the defect (R_{ct}), constant phase element of the double layer at the metal/solution interface of the defect (Q_{dl}) and the constant phase element of the protective film (Q_f). The fitted lines match well to the experimental plots (Figs. 3 a), b) and c)), and all the experimental spectra can be well described by the mentioned equivalent circuit. The protective Zn-layer formed on the immersed specimens may have some defects that led to the formation of pits [35]. The magnitude of impedance signifies the corrosion resistance of steel [20-23, 26, 27]. From Fig. 3 a), it is found that the Zn-rich solution (Zn_{Sol-H}) shows the highest and the Na_{Sol} shows the lowest impedance among the used solutions.

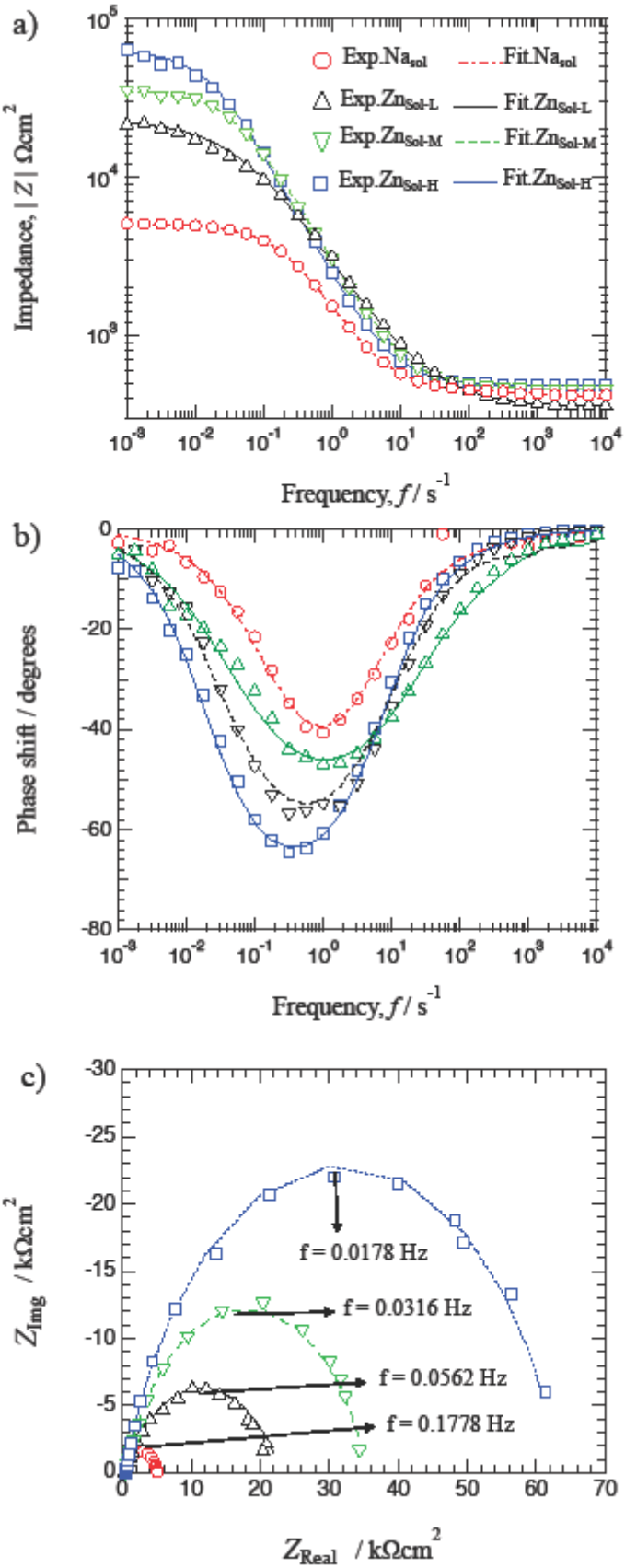

Fig. 3 Bode diagram of a) impedance, b) phase shift plot and c) Nyquist plot of specimen immersed in the solutions for 1 h at room temperature.

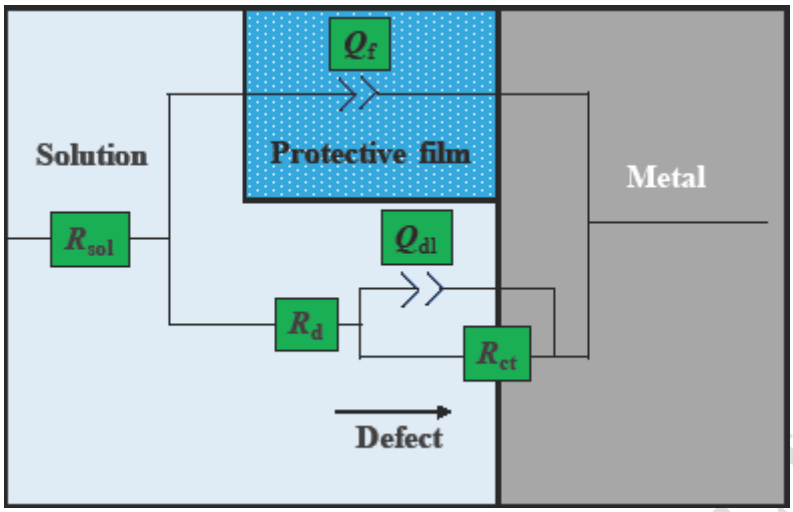

Fig. 4 Equivalent circuit of mild steel electrode with a protective film having defect to fit the EIS data.

The largest phase shift is detected in Zn-rich solution as compared to the other solutions (Fig. 3 b)). From the Nyquist plot (Fig. 3 c)), semicircle plots are observed in all the solutions. However, the radius of the semicircle is increased with increasing the Zn^{2+} concentration.

The electrochemical impedance parameters are shown in Table 1.

Table 1. Calculated electrochemical impedance parameters of mild steel after immersion in the solutions for 1 h at room temperature.

Solutions	R_d ($k\Omega cm^2$)	R_{ct} ($k\Omega cm^2$)	Q_{dl} ($\mu s^n \Omega^{-1} cm^{-2}$)	n_{dl}	Q_f ($\mu s^n \Omega^{-1} cm^{-2}$)	n_f	R_c ($k\Omega cm^2$)	η (%)
Na_{sol}	0.10	4.95	3.34	0.71	3.50	0.69	5.05	-
Zn_{Sol-L}	0.12	21.00	1.19	0.71	1.02	0.72	21.12	76
Zn_{Sol-M}	0.13	37.50	0.98	0.74	0.99	0.72	37.63	87
Zn_{Sol-H}	0.15	62.50	0.85	0.75	0.78	0.73	62.65	92

The corrosion resistance (R_c) and the inhibition efficiency (η) were calculated by the Eqs. (1) and (2):

$$R_c = R_d + R_{ct} \quad (1)$$

$$\text{Inhibition efficiency } (\eta\%) = \frac{R_{c\_sol} - R_{c\_ref}}{R_{c\_sol}} \times 100 \quad (2)$$

Where R_{c_sol} and R_{c_ref} are the values of corrosion resistance in the Zn^{2+} containing solutions and in the reference solution (Na_{sol}). From Table 1, it is found that the η and R_c change as follows, Zn_{Sol-H} >

Zn_{Sol-M} > Zn_{Sol-L} > Na_{Sol}. These results indicate that the charge transfer may be prevented by the Zn-layer that was formed on the steel surface and the thickness of the Zn-layer has been calculated based on the EIS data presented in Table 1 by the Eq. (3) [41]:

$$Q_f = \frac{\varepsilon_{Zn} \times \varepsilon_0 \times A_S}{d_{Zn}} \quad (3)$$

Here, Q_f is the constant phase element of the protective film (μFcm^{-2}), ε_{Zn} is the dielectric constant of ZnO (ε_{Zn} = 25.59) between the frequency range 1 mHz and 10 kHz at 300 K [41], ε_0 is the dielectric permittivity of vacuum (8.854 × 10^{-8} μFcm^{-1}), A_S is the area of the surface (cm^2) and d_{Zn} is the thickness of the Zn-layer (cm).

The calculated values of Zn-layer thickness with the Zn^{2+} concentration in the solutions is shown in Fig. 5. In the case of Na_{sol}, the Na-layer may not be formed on the surface. From the surface analysis, it was explained that Na or Na-related compound cannot form a layer on the metal surface [21, 35, 42]. Therefore, it is deliberated that the layer thickness is zero in Na_{sol}. In the case of Zn_{Sol-L}, the thickness of the Zn-layer is about 22 nm and the thickness are increased with increasing the Zn^{2+} concentration (Fig. 5). The Zn-layer may have not shielded the whole surface of the steel sample. The layer may have some defects. Q_{dl} represents the area of defects in the protective film on the steel surface [21, 35, 42, 43]. Otani et al. [35] reported that the decrease in Q_{dl} indicates that Zn^{2+} can decrease the area of defects in the protective film by forming a layer on mild steel in model freshwater. The defect area has been calculated by comparing with the double layer capacitance of Fe (20 μFcm^{-2}) [44-46].

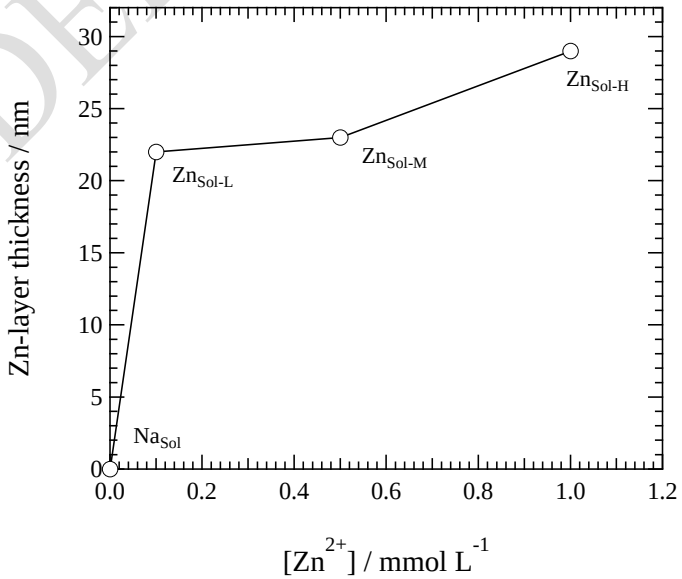

Fig. 5 Thickness of the Zn-layer on the steel surface with Zn^{2+} concentrations.

The calculated values of the defect area with the Zn^{2+} concentration in the solutions is shown in Fig. 6. The area of defects of the film is decreased with increasing the Zn^{2+} concentration. It is assumed that metal dissolution occurs at the defects. Therefore, metal dissolution or corrosion rate is reduced with decreasing the area of the defects. In addition, the resistance at the defect (R_d) is increased (Table 1) with increasing the Zn^{2+} concentration in the solutions, which also indicate that the area of defects may be decreased with increasing the Zn^{2+} concentration. At the high concentration (Zn_{Sol-H}), Zn may have scattered uniformly on the surface and formed a layer that covered the area of the surface more than the area of the surface covered by the other solutions (Zn_{Sol-L} and Zn_{Sol-M}). The uniformed and comparatively thicker layer of Zn^{2+} decreased the defect area that shielded the surface from the aggressive chloride ions hence metal dissolution reactions are inhibited. Consequently, the highest charge transfer resistance was obtained in the Zn-rich solution (Zn_{Sol-H}) as compared to the others.

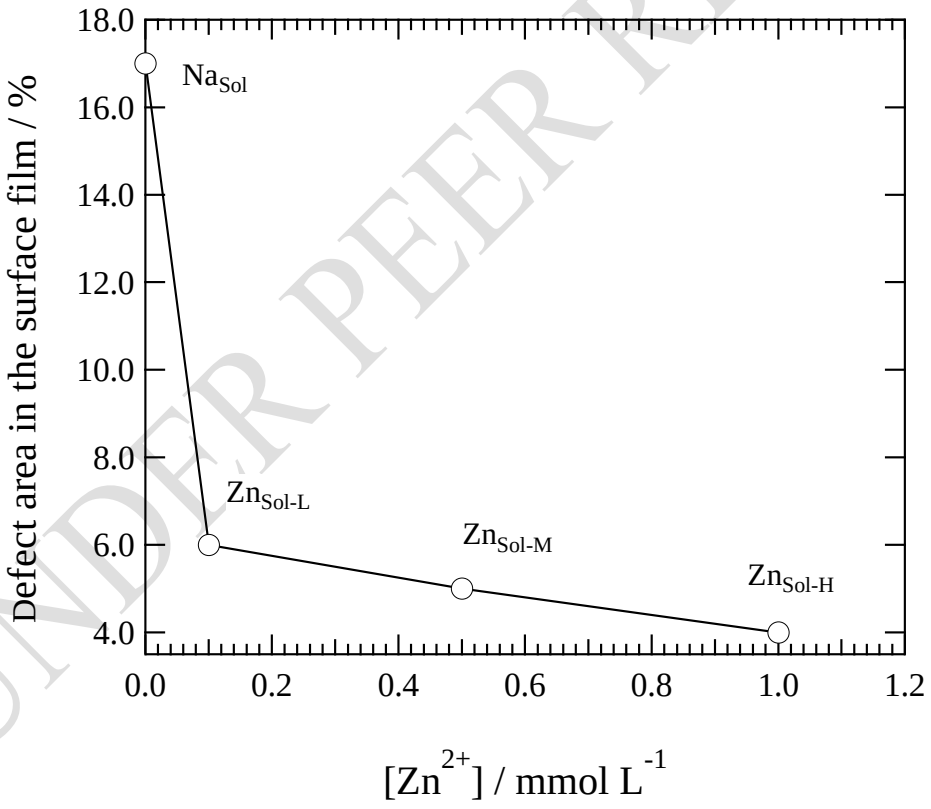

Fig. 6 Defect area of the surface film with Zn^{2+} concentrations.

3.4 R_{ct} and corrosion inhibition efficiency

There is a close relationship between the charge transfer resistance (R_{ct}) and the corrosion rate of steel in solutions.

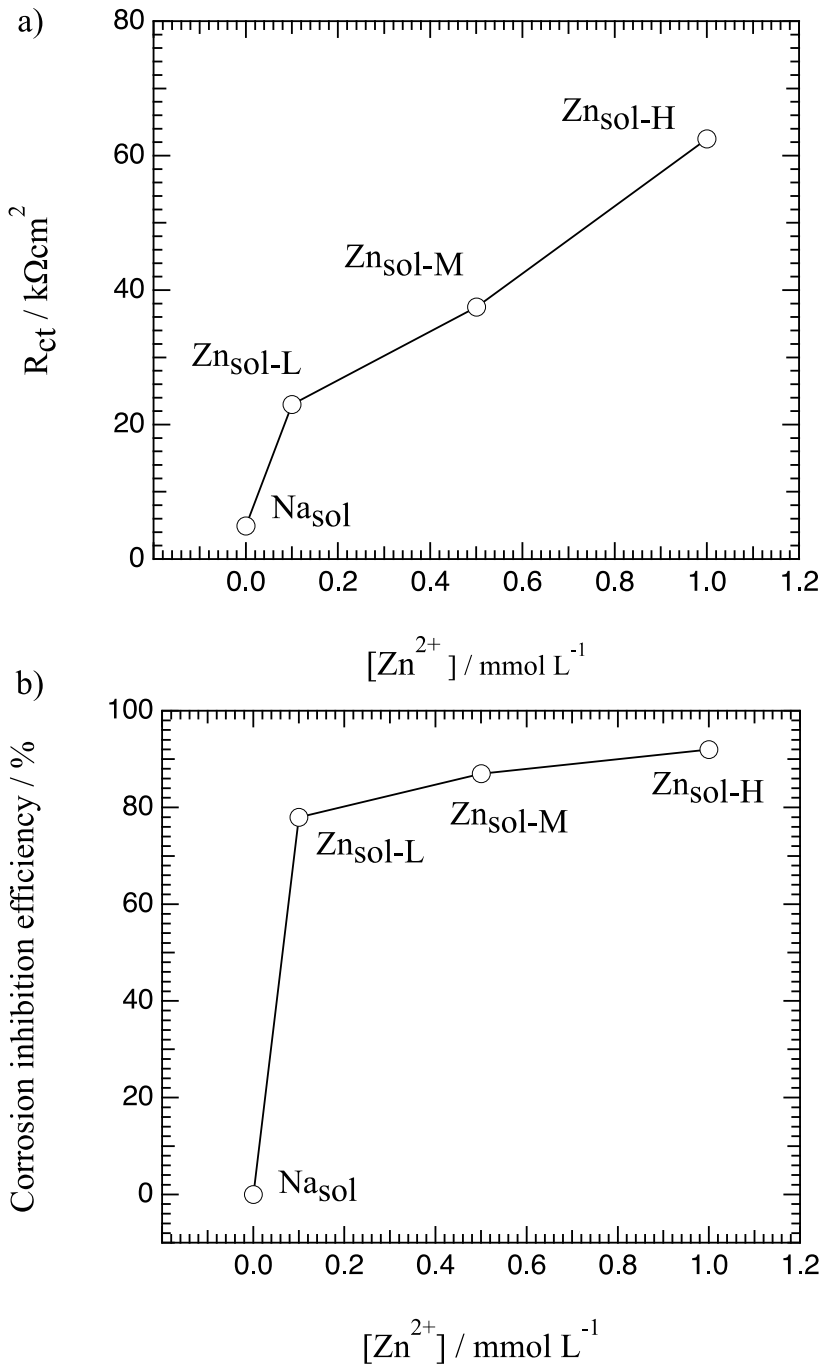

Fig. 7 a) Changes in R_{ct} and b) Corrosion inhibition efficiency as a function of Zn^{2+} concentration in the solutions.

The R_{ct} was calculated, and it was plotted against the Zn^{2+} concentration in the solutions. Fig. 7 a) shows the R_{ct} as a function of Zn^{2+} concentration. R_{ct} is increased with increasing the concentration of Zn^{2+} in the solutions. As it is well known that corrosion resistance is increased with increasing the R_{ct}. These results suggest that the corrosion resistance ability of steel is increased with increasing the

concentration of Zn^{2+} in the solutions. To find out the relation between the corrosion inhibition ability and the Zn^{2+} concentration, corrosion inhibition efficiencies were calculated. Fig. 7 b) shows the corrosion inhibition efficiencies of Zn^{2+} as a function of concentration in which mean values of EIS data were used. The corrosion inhibition efficiency of Na^{+} was considered zero. The inhibition efficiency is increased with increasing the concentration of Zn^{2+}.

3.5 Corrosion inhibition mechanism

Based on the experimental results, a corrosion inhibition mechanism could be suggested. Fig. 8 shows the reaction mechanism of Zn^{2+} with the metal surface film.

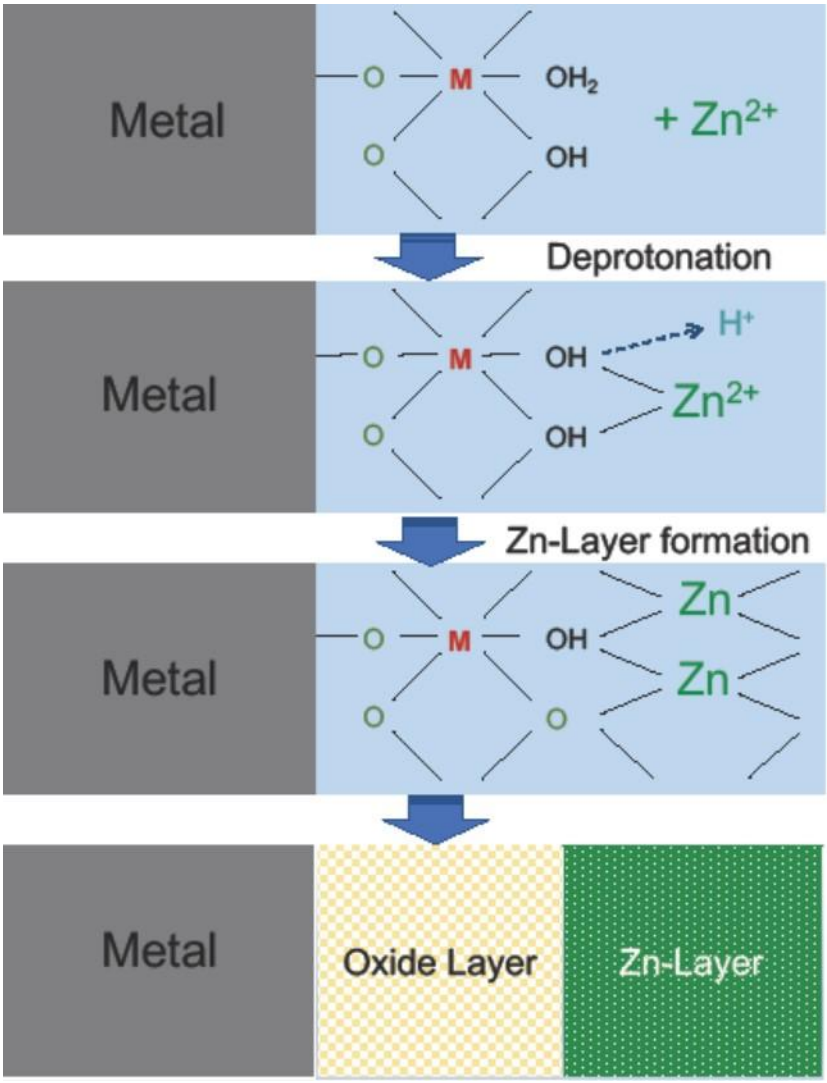

Fig. 8 Reaction mechanism of Zn^{2+} with the metal oxide film and formation of Zn-layer on oxide layer.

In presence of Zn^{2+}, at first deprotonation occurs from the surface film [29]. Then Zn^{2+} forms a bond with the surface film and consequently a network layer is developed. The Zn-layer effectively decreases the defect area of the surface film.

The Zn-layer may be formed both at the cathodic and anodic area and protects the Cl^- attack. As the layer formed at both sites, consequently the layer effectively inhibits the corrosion reactions on the steel surface.

In the case of low concentration of Zn^{2+} ($Zn_{Sol\text{-}L}$), though the Zn-layer is formed, (the thickness of the layer is about 22 nm) the layer may not cover the whole surface. For this reason, Cl^- attack at the defect sites and destroy the surface films and accelerate the metal dissolution (Fig. 9 a)). In the case of medium concentration of Zn^{2+} ($Zn_{Sol\text{-}M}$), Zn-layer thickness is increased and covered the surface more than that in low concentration (Fig. 9 b)). In the case of high concentration ($Zn_{Sol\text{-}H}$), the Zn-layer is uniformed and comparatively thicker (thickness of the layer is about 29 nm) than other solutions ($Zn_{Sol\text{-}L}$ and $Zn_{Sol\text{-}M}$) (Fig. 9 c)). The defect area is decreased by the Zn-layer due to smoothly scattering of Zn^{2+} on the surface and the coverage of the Zn-layer on the surface more than that in $Zn_{Sol\text{-}L}$ and $Zn_{Sol\text{-}M}$ (Fig. 9 c)). Zn-layer with the steel surface protects the chloride ions to destroy the oxide film as well as protects the steel to oxidize. Consequently, the corrosion inhibition efficiency was increased in the Zn-rich solution ($Zn_{Sol\text{-}H}$) as compared to the other solutions.

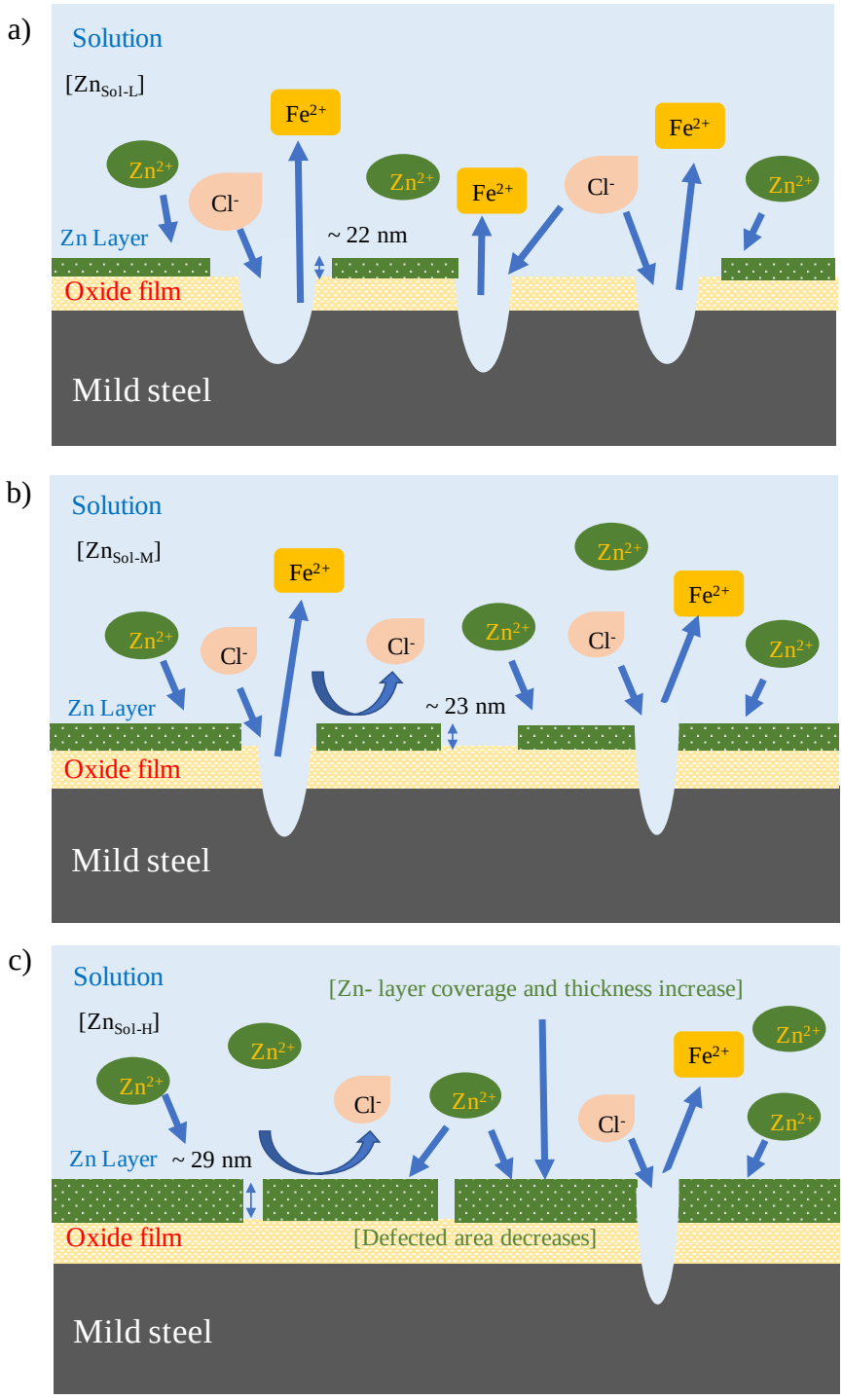

Fig. 9 Corrosion inhibition mechanism by Zn^{2+} at a) low concentration (Zn_{Sol-L}), b) medium concentration (Zn_{Sol-M}), and c) high concentration (Zn_{Sol-H}).

4. CONCLUSION

The corrosion behavior of mild steel in NaCl aqueous solution with different concentration of Zn^{2+} has been investigated by electrochemical tests and the following conclusions can be drawn:

- Zn-rich solution (Zn_{Sol-H}) showed the highest immersion potential as compared to the other solutions.
- Both cathodic and anodic currents were suppressed in the presence of Zn^{2+} in the solutions.
- Charge transfer resistance (corrosion resistance) was increased with increasing the concentration of Zn^{2+} in the solutions.
- Zn^{2+} formed a layer with the steel surface and the thickness of the Zn-layer was increased with increasing zinc ion concentration.
- Zn-rich solution (Zn_{Sol-H}) showed the highest corrosion inhibition efficiency.

REFERENCES

1. Wan Nik WB, Zulkifli F, Rahman MM, Rosliza R. Corrosion behavior of mild steel in seawater from two different sites of kuala terengganu coastal area, *Int. J. Basic & Appl. Sci*. IJBAS-IJENS. 2011; 11 (6): 75-80.
2. Schindelholz E, Risteen BE, Kelly RG. Effect of relative humidity on corrosion of steel under sea salt aerosol proxies, *J. Electrochem. Soc*. 2014; 161 (10): C460-C470. http://dx.doi.org/10.1149/2.0231410jes.
3. Morcillo M, Chico B, Alcantara J, Diaz I, Wolthuis R, De la Fuente D. SEM/Micro-Raman characterization of the morphologies of marine atmospheric corrosion products formed on mild steel, *J. Electrochem. Soc*. 2016; 163 (8): C426-C439. http://dx.doi.org/10.1149/2.0411608jes.
4. Amin MA, Ibrahim MM. Corrosion and corrosion control of mild steel in concentrated H_2SO_4 solutions by a newly synthesized glycine derivative, *Corros. Sci*. 2011; 53 (3): 873-885. http://dx.doi.org/10.1016/j.corsci.2010.10.022.
5. Prabhu RA, Venkatesha TV, Shanbhag AV, Kulkarni GM, Kalkhambkar RG. Inhibition effects of some schif's bases on the corrosion of mild steel in hydrochloric acid solution, *Corros. Sci*. 2008; 50: 3356-3362. http://dx.doi.org/10.1016/j.corsci.2008.09.009.
6. Soliz A, Caceres L. Corrosion of a carbon steel cylindrical band exposed to a concentrated NaCl solution flowing through an annular flow cell, *J. Electrochem. Soc*. 2015; 162 (8): C385-C95. http://dx.doi.org/10.1149/2.0201508jes.

7. Khara S, Choudhary S, Sangal S, Mondal K. Corrosion resistant Cr-coating on mild steel by powder roll bonding, *Surf. Coat. Technol*. 2016; 296: 203-210. http://dx.doi.org/10.1016/j.surfcoat.2016.04.033.

8. Gardiner CP, Melchers RE. Corrosion of mild steel by coal and iron ore, *Corros. Sci*. 2002; 44: 2665-2673. http://dx.doi.org/10.1016/S0010-938X(02)00063-X

9. Ahamed KR, Farzana BA, Diraviam SJ, Dorothy R, Rajendran S, Al-Hashem A. Mild steel corrosion inhibition by the aqueous extract of commelina benghalensis leaves, *Electrochim. Acta* 2019; 37 (1): 51-70. http://dx.doi.org/ 10.4152/pea.201901051.

10. Medrano-Vaca MG, Gonzalez-Rodriguez JG, Nicho ME, Casales M, Salinas-Bravo VM. Corrosion protection of carbon steel by thin films of poly (3-alkyl thiophenes) in 0.5 M H_2SO_4, *Electrochim. Acta* 2008; 53 (9): 3500-3507. http://dx.doi.org/10.1016/j.electacta.2007.12.003.

11. Hassan HH, Abdelghani E, Amin MA. Inhibition of mild steel corrosion in hydrochloric acid solution by triazole derivatives part I. polarization and EIS studies, *Electrochim. Acta* 2007; 52 (22): 6359-6366. http://dx.doi.org/10.1016/j.electacta.2007.04.046.

12. Veloz MA, Gonzalez I. Electrochemical study of carbon steel corrosion in buffered acetic acid solutions with chlorides and H_2S, Electrochim. Acta 2002; 48 (2):135-144. http://dx.doi.org/10.1016/S0013-4686(02)00549-2.

13. Krstajic NV, Grgur BN, Jovanovic SM, Vojnovic MV. Corrosion protection of mild steel by polypyrrole coatings in acid sulfate solutions, *Electrochim. Acta* 1997; 42 (11): 1685-1691. https://doi.org/10.1016/S0013-4686(96)00313-1.

14. Zhou Q, Sheikh S, Ou P, Chen D, Hu Q, Guo S. Corrosion behavior of $Hf_{0.5}Nb_{0.5}Ta_{0.5}Ti_{1.5}Zr$ refractory high entropy in aqueous chloride solutions, *Electrochem. Commun*., 2019; 98: 63-68. https://doi.org/10.1016/j.elecom.2018.11.009.

15. Foley RT. Role of the chloride ion in iron corrosion, *Corros*ion 1970; 26 (2): 58-70. https://doi.org/10.5006/0010-9312-26.2.58.

16. Macdonald DD. The point defect model for the passive state, *J. Electrochem. Soc*. 1992; 139 (12): 3434-3449. https://doi.org/10.1149/1.2069096.

17. McCafferty E., *Introduction to Corrosion Science*, Springer, New York; 2010: 283-286. https://doi.org/10.1007/978-1-4419-0455-3.

18. Deyab MA. Electrochemical investigations on pitting corrosion inhibition of mild steel by provitamin B5 in circulating cooling water, *Electrochim. Acta* 2016; 202: 262-268. https://doi.org/10.1016/j.electacta.2015.11.075.

19. Song Y, Jiang G, Chen Y, Zhao P, Tian Y. Effects of chloride ions on corrosion of ductile iron and carbon steel in soil environments, *Scientific reports*, 2017; 7 (1). https://doi.org/10.1038/s41598-017-07245-1.

20. Otani K, Sakairi M. Effects of metal cations on corrosion of mild steel in model fresh water *Corros. Sci*. 2016; 111: 302-312. https://doi.org/10.1016/j.corsci.2016.05.020.

21. Islam Md.S, Otani K, Sakairi M. Effects of metal cations on mild steel corrosion in 10 mM Cl^- aqueous solution, *Corros. Sci*. 2018; 131: 17-27. https://doi.org/10.1016/j.corsci.2017.11.015.

22. Islam Md.S, Otani K, Sakairi M. Role of metal cations on corrosion of coated steel substrate in model aqueous layer, *ISIJ International* 2018; 58 (9): 1616-1622. https://doi.org/10.2355/isijinternational.ISIJINT-2018-071.

23. Islam Md.S, Otani K, Sakairi M. Corrosion inhibition effects of metal cations on SUS304 in 0.5 M Cl^- aqueous solution, *Corros. Sci*. 28; 140: 8-17. https://doi.org/10.1016/j.corsci.2018.06.028.

24. Prawoto Y, Ibrahim K, Nik WBW. Effect of pH and chloride concentration on the corrosion of duplex stainless steel, Arabian J. Sci. Eng., 2009; 34 (2C): 115-127. http://dx.doi.org/10.1016/j.jmrt.2016.11.001.

25. Song Y, Jiang G, Chen Y, Zhao P, Tian Y. Effects of chloride ions on corrosion of ductile iron and carbon steel in soil environment, *Scientific Report*, 2017; 7 (1):6865. http://dx.doi.org/10.1038/s41598-017-07245-1.

26. Otani K, Sakairi M, Sasaki R, Kaneko A, Seki Y, Nagasawa D. Effect of metal cations on corrosion behavior and surface film structure of the A3003 aluminum alloy in model tap waters, *J. Solid State Electrochem*. 2014; 18 (2): 325-332. https://doi.org/10.1007/s10008-013-2260-7.

27. Islam Md.S, Sakairi M. Effects of Zn^{2+} concentration on the corrosion of mild steel in NaCl aqueous solutions *J. Electrochem. Soc.* 2019; 166 (2): C83-C90. https://doi.org/10.1149/2.1271902jes.

28. Drazic DM, Vorkapic LZ. Inhibitory effects of manganeous, cadmium and zinc ions on hydrogen evolution reaction and corrosion of iron in sulphuric acid solutions, *Corros. Sci*. 1978; 18 (10): 907-910. https://doi.org/10.1016/0010-938X(78)90011-2.

29. Zhang S, Shibata T, Haruna T. Inhibition effect of metal cations to intergranular stress corrosion cracking of sensitized type 304 stainless steel, *Corros. Sci*. 2005; 47 (4): 1049-1061. https://doi.org/10.1016/j.corsci.2004.06.014.

30. Felhosi I, Keresztes Zs, Karman FH, Mohai M, Bertoti I, Kalman E. Effecrts of bivalent cations on corrosion inhibition of steel by 1-hydroxyethane-1, 1-diphosphonic acid, *J. Electrochem. Soc*. 1999; 146 (3): 961-969. https://doi.org/10.1149/1.1391706.

31. Telegdi J, Shaglouf MM, Shaban A, Karman FH, Betroti I, Mohai M, Kalman E. Influence of cations on the corrosion inhibition efficiency of aminophosphonic acid, *Electrochim. Acta* 2001; 46 (24): 3791-3799. https://doi.org/10.1016/S0013-4686(01)00666-1.

32. Sathiyanarayanan S, Jeyaprabha C, Muralidharan S, Venkatachari G, Inhibition of iron corrosion in 0.5 M sulphuric acid by metal cations, *App. Surf. Sci*. 2006; 252 (23): 8107-8112. https://doi.org/10.1016/j.apsusc.2005.10.028.

33. Zhang DQ, Cai QR, He XM, Gao LX, G. S. Kim GS. Corrosion inhibition and adsorption behavior of methionine on copper in HCl and synergistic effect of zinc ions, *Mater. Chem. Phys*. 2009; 114 (2-3): 612-617. https://doi.org/10.1016/j.matchemphys.2008.10.007.

34. Prabakaran M, Venkatesh M, Ramesh S, Periasamy V. Corrosion inhibition behavior of propyl phosphonic acid-Zn^{2+} system for carbon steel in aqueous solution, *App. Surf. Sci*. 2013; 276 : 592-603. https://doi.org/10.1016/j.apsusc.2013.03.138.

35. Otani K, Islam Md.S, Sakairi M. Inhibition ability of gluconates for freshwater corrosion of mild steel enhanced by metal cations, *J. Electrochem. Soc.* 2017; 164 (9): C498-C504. https://doi.org/10.1149/2.0491709jes.

36. Thebault F, Vuillemin B, Oltra R, Allely C, Ogle K, Heintz O. Influence of magnesium content on the corrosion resistance of the cut-edge of Zn-Mg-coated steel, *Corros. Sci.* 2015; 97: 100-106. https://doi.org/10.1016/j.corsci.2015.04.019.

37. Tada E, Satoh S, Kaneko H. The spatial distribution of Zn^{2+} during galvanic corrosion of a Zn/steel couple, *Electrochim. Acta* 2004; 49 (14): 2279-2285. https://doi.org/10.1016/j.electacta.2004.01.008.

38. Sakairi M, Uchida Y, Yoshiyuki H. Initial stage of localized corrosion in artificial pits formed with photon rupture on 55mass%Al-Zn coated steels, *ISIJ International.* 2006; 46 (8): 1218-1222. https://doi.org/10.2355/isijinternational.46.1218.

39. Hirasaki T, Nishikata A, Tsuru T. Influence of dissolved zinc ions on the anodic dissolution of iron, *J. Japan Inst. Metals*. 2002; 66 (6): 643-648. https://doi.org/10.2320/jinstmet1952.66.6_643.

40. Vacandio F, Massiani Y, Gergaud P, Thomas O. Stress porosity measurements and corrosion behavior of AIN films deposited on steel substrates, *Corros. Sci*. 2000; 359 (2): 221-227. https://doi.org/10.1016/S0040-6090(99)00763-4.

41. Lanje AS, Sharma SJ, Ningthoujam RS, Pode RB. Low temperature dielectric studies of zinc oxide (ZnO) nanoparticles prepared by precipitation method. *Adv. Powder Technol*., 2013; 24 (1): 331-335. https://doi.org/10.1016/j.apt.2012.08.005.

42. Islam Md.S, Sakairi M. Corrosion inhibition of mild steel by metal cations in high pH simulated freshwater at different temperatures. *Corros. Sci*. 2019; 153: 100-108. https://doi.org/10.1016/j.corsci.2019.03.040.

43. Mahdavian M, Naderi R. Corrosion inhibition of mild steel in sodium chloride solution by some zinc complexes, *Corros. Sci*. 2011; 53 (4):1194-1200. https://doi.org/10.1016/j.corsci.2010.12.013.

44. Bokris JOM, Reddy AKN. Modern Electrochemistry, Vol. 1 and 2, Plenum (1973).

45. Adams RN. Electrochemistry at solid electrode, Marcel Dekker, New York, (1969). https://doi.org/10.1002/bbpc.19690731029.

46. Bard AJ, Lund H. Encyclopedia of the Electrochemistry of the elements, Marcel Dekker, New York (1971-1980).